



# An Information-Based World-Earth System Resilience Index

John M. Anderies<sup>1,\*</sup>, Max Bechthold<sup>2,3,4,\*</sup>, Jonathan F. Donges<sup>2,4,5</sup>, Ingo Fetzer<sup>3,6</sup>, Nico Wunderling<sup>2,7</sup>,  
Wolfram Barfuss<sup>2,8,9</sup>, and Johan Rockström<sup>2,5,10</sup>

<sup>1</sup>School of Sustainability and School of Human Evolution and Social Change, Arizona State University, Tempe, AZ 85287, USA

<sup>2</sup>Earth Resilience Science Unit, Potsdam Institute for Climate Impact Research, Member of the Leibniz Association, Telegrafenberg A31, D-14473 Potsdam, Germany

<sup>3</sup>Institute of Physics and Astronomy, University of Potsdam, D-14476 Potsdam, Germany

<sup>4</sup>Department Integrative Earth System Science, Max Planck Institute of Geoanthropology, Kahlaische Strasse 10, D-07745 Jena, Germany

<sup>5</sup>Stockholm Resilience Centre, Stockholm University, Frescativägen 8, SE-106 91 Stockholm, Sweden

<sup>6</sup>Bolin Centre for Climate Research, Stockholm University, Stockholm, Sweden

<sup>7</sup>Center for Critical Computational Studies, Goethe University Frankfurt, D-69629 Frankfurt am Main, Germany

<sup>8</sup>Center for Development Research (ZEF), University of Bonn, Genscherallee 3, D-53113 Bonn, Germany

<sup>9</sup>Institute for Food and Resource Economics, University of Bonn, Genscherallee 3, D-53113 Bonn, Germany

<sup>10</sup>Institute of Environmental Science and Geography, University of Potsdam, D-14476 Potsdam, Germany

\*The first two authors share the lead authorship.

**Correspondence:** Max Bechthold (maxbecht@pik-potsdam.de)

**Abstract.** In order to address the emerging global polycrisis, it is essential to develop quantitative indicators for estimating resilience of essential bio-geophysical and social drivers of change. Such indicators are required to navigate the Anthropocene and to assess which actions increase the likelihood of achieving a safe and just operating space (SAJOS). In this paper, we propose a novel information-based resilience metric. We define it as the conditional probability of a system reaching a desired system state, e.g. a SAJOS, given initial conditions and an information set. This information set reflects knowledge about relevant ranges of bio-physical and socio-cultural system dynamics, boundaries and perturbations. The resulting resilience index is highly dependent on the available information about the system and its intrinsic action capacities. An increase in epistemic knowledge about the system does not necessarily result in enhanced resilience. It is still possible to envisage scenarios in which one could find oneself in a world that is capable of attaining a SAJOS in only a limited number of circumstances. Our proposed approach facilitates the operationalization and quantification of resilience in complex World-Earth system (WES) models. Resilience should be understood as being constrained by available information about the system, its internal processes, boundaries, and the capacity of the system to act in an uncertain future. This further implies the importance of making informed investment decisions that balance improving system understanding (i.e. gaining information), increasing (anticipatory) capacities of action, and taking common-sense action to enhance resilience. Our information-based index can be applied to any kind of system. Since it answers the classical question of “resilience of what, to what” on a meta level, it allows moving beyond a highly specified and static notion of resilience, allowing for a wide range of application cases.



## 1 Introduction

The concept of resilience has been gaining traction in a number of fields related to environmental change as a potentially useful concept for setting goals (Folke et al., 2010; Scheffer et al., 2015) such as poverty alleviation (Lade et al., 2017) or building  
20 community resilience (e.g. Berkes and Ross (2013)) and more specific policy applications such as designing institutions to govern for resilience in SES (e.g. Lebel et al. (2006); Barfuss et al. (2018); Milkoreit et al. (2018); Milkoreit (2025)). However, a policy-relevant definition of resilience remains elusive. The challenge of developing policy-relevant notions of resilience stems from several factors. First, resilience is a system-level concept that characterizes the dynamics of nonlinear dynamical systems involving advanced mathematical understanding (Krakovská et al., 2024), typically beyond the scope of practical  
25 policy action. Second, resilience is used in various ways in the literature to refer broadly to the capacity of some entity to “bounce back” from a “shock” or “perturbation” (Folke et al., 2010). Although an appealing idea, the entity in question, the nature of the shock, and the nature of the process of bouncing back are often vaguely defined. The questions of what capacity, what entity, what shock, and what bouncing back looks like are rarely defined with enough precision to generate practical policy utility. Third, because resilience is a complex systems concept, defining easy-to-understand metrics for resilience is difficult  
30 (Anderies et al., 2013b; Baird et al., 2024; Franco-Gaviria et al., 2022; Tamberg et al., 2022). Finally, given the challenges of characterizing different forms of uncertainty (initial condition, parametric, structural or aleatoric, epistemic, etc.) and its relation to decision-making, notions of resilience of practical decision-making utility remain underdeveloped. Therefore, we need concepts beyond the well-known notions of persistence resilience, adaptation resilience and transformation resilience (e.g. Folke et al. (2010)).

35 Given the rapid progression of climate change and globalization, resilience has entered the discourse around global change, e.g., the notions of Earth system resilience (Anderies et al., 2013a; Rockström et al., 2021, 2023; Steffen et al., 2018) and World-Earth system resilience (Anderies et al., 2023), which underlie science-policy frameworks such as the planetary boundaries and Earth system boundaries frameworks (Milkoreit, 2025; Richardson et al., 2023; Rockström et al., 2023). The more degrees of freedom in the system under study - that is, the higher the number of independent ways it can change - and the  
40 deeper the uncertainties involved, the more difficult resilience analysis becomes. Early studies of resilience in social-ecological systems focused on reasonably well-bounded and well-understood systems, e.g., shallow lakes (Carpenter and Cottingham, 1997; Scheffer et al., 1993; Scheffer and Carpenter, 2003; Scheffer and Van Nes, 2007), rangelands (Anderies et al., 2002), and thus could extract reasonably well-defined characterizations of resilience. In such studies, the “resilience of what to what” (Carpenter et al., 2001; Tamberg et al., 2022) question could be answered, i.e., the resilience of the oligotrophic regime of  
45 a shallow lake to phosphorus loading or the resilience of a mixed grass-shrub regime in a fire-driven rangeland to grazing pressure. For resilience analysis to be concrete, measurable, and relevant, answering this question is crucial. However, in the current Anthropocene epoch many global processes are no longer driven only by a geo-biophysical “Earth system” but also by the aggregation of social decisions manifested globally in a human “World system”, e.g. carbon emissions, land use change, biodiversity loss and other (Beckage et al., 2018; Crutzen, 2002; Edwards, 2015; Schellnhuber, 1999). Given the high complexity of a “World-Earth system” (WES), i.e., a planet with the capacity to support life on which an organism capable of  
50

organizing a complex network of societies has emerged with enormous information, energy, and material processing capacity, operationalizing and quantifying resilience is an entirely different challenge.

In this study, we extend an existing World-Earth model (Fig. 1A) to provide guidance on how to develop an aggregate metric of World-Earth system resilience, an index, to estimate the remaining buffering capacity of the global social-ecological system towards shocks and adaptability to changes that can be meaningfully used in policy processes. Our approach hinges on the importance of uncertainty and, more precisely, on the role of information and agency in determining the resilience of a system (Brown and Westaway, 2011; Donges and Barfuss, 2017). We outline our approach in detail in the Theory and Methods, Sect. 2, but the essence is straightforward: The information-based resilience index we develop is the conditional probability of reaching a desired system regime given an initial system state and an information set. This conditional probability incorporates traditional topological elements of resilience (the geometry of basins of attraction generated by tipping elements, tipping cascades, etc.), the interaction of very fast, fast, and slow dynamics (very fast = e.g. extreme weather events such as floods, heat waves and hurricanes, fast = system drivers such as recent carbon emissions, slow = e.g., increase in atmospheric carbon stocks), and the potential of human agency. In this study, agency is based on the idea of controllability which characterizes relevant actors' capacities to navigate through the topological landscape defined by fast and slow dynamics while being buffeted by high-frequency shocks (very fast dynamics) to remain in or move between different basins of attraction.

Our focus on an information-based resilience index (IBRI), framed as an intuitive conditional probability, is strongly motivated by the need to provide tools for practical policy action and offer clear guidance on which interventions best support desirable system outcomes. A resilience index is most useful if it can inform a recursive decision-making process in a dynamical system, in our case the World-Earth system. More specifically, it should be a useful, practical signal in a coevolutionary feedback control process embedded in the complex, self-organizing, coupled World-Earth system (Beckage et al., 2018; Donges et al., 2017, 2020). Unlike theoretical mathematical characterizations of resilience based on the topology of potential fields (Hellmann et al., 2016; Van Kan et al., 2016; Menck et al., 2013; Scheffer et al., 2009; Schultz et al., 2017; Yi et al., 2025), the information-based index acts as a tool to translate what policy actors think they know (e.g., their priors) into a single number using conditional probability as discussed above. This may drive policy actors to reflect on what they think they know and point to the most important areas where uncertainty must be reduced. It may also help reconcile different narratives and beliefs of policy actors engaged in collective decision-making and accelerate the pace of collective action required to address challenges in the World-Earth system.

In this work we illustrate the capabilities of the information-based resilience index as a tool to assess resilience of real-world systems by rigorously including the inherent uncertainties of these systems and the modeling process. The contribution of this paper is twofold: first, the concept and (mathematical) formalization of the information-based resilience index is elaborated (Sect. 2), including a brief description of the World-Earth simulation model used for formalization (Sect. 2.1). Second, the index is used to assess a deterministic and stochastic version of this model (Sect. 3), showing its interpretational and informational power. Finally, Sect. 4 concludes the paper. The most significant contribution of the paper is to illustrate what decision makers think they know critically impacts resilience, leads to different resilience measures for each decision maker and how these



85 various resilience measures may feed into collective decision processes. Our index can therefore help to bound belief systems  
and offers a narrative opportunity to focus on change rather than current states.

## 2 Theory and methods

While there is a large literature on building theory around the notion of resilience (see e.g. Yi et al. (2025) for a recent review),  
there are certain elements of a theory of resilience that are often not made explicit in the governance of SES/environmental  
90 policy literatures that are important to highlight for our study:

1. Social-ecological resilience (as opposed to engineering resilience) is fundamentally based on the existence of multiple at-  
tractors (subregions of state space) in a nonlinear dynamical system, generated by the interaction of fast(er) and slow(er)  
processes within the system. Thus, while resilience is a ‘system-level’ concept, it makes little sense to refer to ‘resilient  
systems’ or ‘system resilience’ because resilience refers to characteristics of attractors within a system, i.e., to subsets  
95 of the system state space, not the entire system. The one exception here may be the case that a system is globally stable,  
i.e., there is a single attractor for the system. In that case, the system is “perfectly resilient” (in contrast, engineering  
resilience measures the rate of return to an equilibrium state even in this case). Thus, in this study, World-Earth System  
resilience refers to particular (desirable) attractors in the state space of all possible World-Earth system attractors.
2. A policy-relevant notion of resilience must make explicit all relevant processes and time scales present in the system  
100 in question and identify those that are actionable, i.e., answering the ‘resilience of what to what’ question (Carpenter  
et al., 2001). Furthermore, what is considered the system being acted upon and the control system (e.g., the sensor-  
action-response loop) acting on that system must be distinguished. This distinguishes resilience theory from viability  
theory (Martin, 2004), highlights the importance of agency, and has practical implications for problem framing and  
communication of any resilience index. We discuss this further below.
- 105 3. Building on points 1 and 2, a practical, policy-relevant resilience concept should combine elements of information,  
agency, and traditional notions of topological resilience (the ball-and-cup metaphor).

These three theoretical considerations/axioms form the basis of our information-based resilience index. To build up our  
index, we begin with the traditional framework for topological resilience as depicted in Fig. 1B that appears very frequently in  
the research literature. On top of this framework, we add fluctuations and the capacity for control. The safe (left, light grey)  
110 and unsafe (right, dark grey) operating spaces are shown. The notion of resilience in the classic framework is often understood  
as the distance between the branch of desirable equilibria at the top (note that justice considerations - i.e. how desirable is  
defined - may move the equilibria along this branch and thus have implications for resilience) and the branch of unstable  
equilibria (dashed) for a given value of the slower variable, as shown by the red arrow. We refer to this as topological resilience  
(of the safe operating space) and define it as the maximum perturbation in the fast(er) variable the (uncontrolled) system can  
115 tolerate before moving into the unsafe operating space. For a detailed overview of resilience concepts and their mathematical  
foundations, see Krakovská et al. (2024).

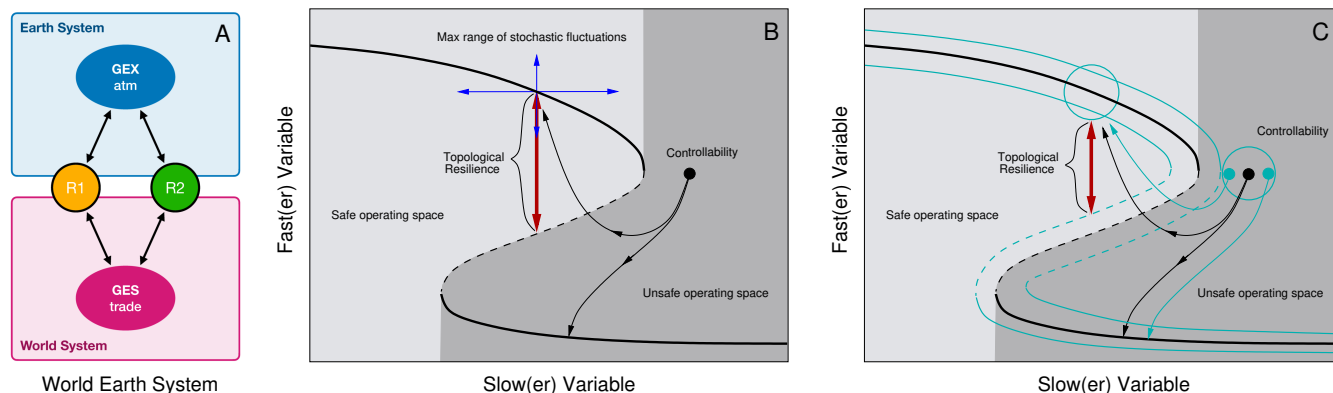


**Figure 1.** A) Schematic of the two-region World-Earth System analyzed here. World-Earth systems are created by regions connected by globalized infrastructure such as trade or information networks that create a global economic system (GES) which are in turn connected to the Earth system via a global process (GEX) such as the atmospheres. See Anderies et al. (2023) for a comprehensive treatment of the World-Earth system concept. B) Standard depiction of resilience and tipping points. The solid and dashed curves represent stable and unstable equilibria, respectively. We assume the upper branch of equilibria are desirable. C) The importance of information for the notion of resilience. Cyan entities illustrate limited knowledge and limited measurement capabilities.

The vertical and horizontal blue arrows represent the maximum variation in the fast(er) and slow(er) variables, respectively, and capture the notion of stochastic resilience. Stochastic resilience is defined as the probability that the system will not transition from the desirable regime to the undesirable regime and is thus represented by the joint probability distribution of this transition. Note that in the example in the Fig. 1, the maximum range stochastic fluctuation is within the SOS so the probability of this transition is equal to zero and thus stochastic resilience is equal to 1 (the desirable regime is perfectly resilient). Imagine now that the slow(er) variable, e.g. atmospheric greenhouse gas concentrations, is increasing, and the blue arrows are moving to the right along the upper branch. Eventually, the topological resilience will become smaller than the range of stochastic variation, and stochastic resilience will drop below a value of 1.

Stochastic resilience thus defined corresponds to Earth System resilience: for a given value of the slow variable (slow variables are treated as parameters in resilience studies) such as atmospheric carbon concentration, the Earth System can tolerate a specific range of variation. Such an index does not incorporate human agency beyond the fact that it may (typically passively) impact the value of the slow(er) variable and change Earth system resilience. Active human agency has two key elements: 1) access to information and knowledge to inform how to act and 2) capacity to translate a decision to act into actual action (e.g. move the slow variable to the left). In Fig. 1B, agency is incorporated through controllability. Agents can act to drive the system back to the safe operating space, if they act soon enough and strongly enough to overcome the topological dynamics. This incorporation of agency into our analysis adds the element of World system resilience to Earth system resilience. The impact of knowledge and measurement capacity on agency is depicted in Fig. 1C. (reflected as uncertainty bounds and measurement limitations by the cyan curves in the Fig.) . Actors in the system may not have a complete understanding of the underlying topology, such as the location of attractor boundaries. Moreover, they may not be able to accurately measure the state of the



system and thus assess their location in a given attractor. In this case, an information-adjusted value of topological resilience can be calculated as the minimum distance between possible system states and basin boundaries. Whereas in Fig. 1B, the importance of stochastic fluctuations (a kind of uncertainty) and controllability for resilience is emphasized, Fig. 1C highlights the importance of more fundamental information limitations on resilience. Combining all of these processes to assess combined World-Earth system resilience requires a pathwise perspective. That is, we need to assess all possible pathways for the dynamics of the system given a certain characterization of system information, i.e. how much is known about the system and the capacity to measure and steer it and assign a resilience index to this bundle of paths.

## 2.1 Model

To operationalize the IBRI, some sort of model (conceptual, computational, statistical, mathematical, or otherwise) that reflects understanding (with attendant characterization of uncertainties) of the system in question is required. We have chosen to operationalize the IBRI using the World-Earth system model as presented and specified in Anderies et al. (2023), without migration. This model captures a World of  $N$  regions (we set  $N = 2$  in our analysis here) with human population dynamics  $P$ , capital fluxes  $K$ , and economic production infrastructure. The Earth system is represented by a global (e.g. atmospheric carbon) externality  $G$  that introduces damages and a stylized tipping element (e.g. Amazon rainforest dieback or permafrost thaw), i.e. a positive feedback in the global externality once a threshold  $G_0$  is passed (see e.g. Armstrong McKay et al. (2022) and Lenton et al. (2025)).

This model strikes a balance between capturing biophysical, social, and economic processes and the appropriate level of complexity for a resilience analysis. The interaction between the regions is governed by the Earth system externality that impacts (e.g. extreme weather events) World systems economies and the capacity of the World system to manage the externality through coordination.

The dynamics of the model are captured by the dynamical system

$$\frac{dP_j}{dt} = r_j P_j \left( 1 - \frac{P_j}{\kappa_j} \right), \quad (1)$$

$$\frac{dK_j}{dt} = I_j - \delta_j K_j - \sigma_j S_j(G) K_j, \quad (2)$$

$$\frac{dG}{dt} = e_1(t) Y_{i1} + e_2(t) Y_{i2} - u(G - G_e) + \theta(G - G_0), \quad (3)$$

where  $j \in \{1, 2\}$  denotes the different regions and their parametrization. Parameters  $\kappa_j$  and  $r_j$  denote intrinsic growth rate and carrying capacity of the population,  $\delta_j$  the depreciation of built infrastructure,  $\sigma_j$  the scaling of climate damages  $S_j(G)$  that depend on the global externality. Capital stocks  $K_j$  increase with investment  $I_j$ . The parameter  $u$  represents the intrinsic assimilation capacity for  $G$  (e.g. carbon sequestration by marine and terrestrial systems), respectively.  $G$  is the global externality, e.g. atmospheric carbon concentration, and is increased via emissions  $e$  from economic output  $Y$ .  $G_e$  is the carbon concentration toward which the ES will tend within a given climate regime in the absence of anthropogenic forcing, e.g.  $G_e = 280$  ppm based on pre-industrial levels. Economic output is given by  $Y_j = \max\{Y_{bj}, Y_{ij}\}$  where  $Y_{bj}$  is a "backstop", very low emission



technology and  $Y_{ij}$  is much higher emission industrial technology modeled using the standard Cobb-Douglas technology:

$$Y_{ij} = A_j K_j^{\alpha_j} L_j^{\beta_j}, \quad (4)$$

with  $L_j$  and  $A_j$ , the labor supply and total factor productivity with constant returns to scale ( $\alpha_j + \beta_j = 1$ ). We assume full  
 170 employment so  $L = P$ . When a decarbonization threshold  $T_g$  in ppm is reached, regions begin to decarbonize according to

$$\frac{de_j}{dt} = -z(G, T_g) r_{e,j} e_j, \quad (5)$$

where  $r_{e,j}$  is the decarbonization rate and  $z(G, T_g)$  is a threshold function that switches smoothly from 0 to 1 as  $G$  crosses the  
 threshold. Where not indicated otherwise, we use the standard initial parametrization of the model as shown in Table 1, with an  
 increased Earth system carbon uptake parametrization of  $u = 0.014$ , yielding a more realistic match of  $G$  with historical data.  
 175 Additionally, we assume  $\sigma = \sigma_1 = \sigma_2$  and  $re = re_1 = re_2$  for computational reasons that become apparent in the following  
 Sect. 2.2. For the full derivation and rational of the model beyond the main dynamics shown here (e.g., investment  $I_j$ , backstop  
 technologies, etc.) consult Anderies et al. (2023). We also use the standard initial conditions from Anderies et al. (2023) also  
 shown in Table 1.

**Table 1.** Parameter definitions, units, and default values and initial conditions that are copied from the original Anderies et al. (2023) model. Sources and fits can be found in the original publication. See text for definitions of other parameters that are varied extensively in the analysis.

Parameters			Initial Conditions	
Symbol	Definition/units	Default value	Variable	Initial Condition
$r_1, r_2$	Intrinsic growth rates (1/time)	0.038, 0.042	$K_1$	0
$\kappa_1, \kappa_2$	Carrying capacity ( $10^9$ persons)	1.5, 9.7	$K_2$	0
$\delta_i$	Entropic decay rates (1/time)	0.05	$P_1$	0.24
$e_i$	Emission intensity (hecto ppm/ $10^{12}$ \$)	0.0004	$P_2$	0.24
$A_1, A_2$	Total factor productivity	2.7, 1.7	$e_1$	0.0004
$\beta_1, \beta_2$	Output elasticity/factor share of labor	0.5, 0.5	$e_2$	0.0004
$\alpha_1, \alpha_2$	Output elasticity/factor share of capital	0.5, 0.5	$G$	280

## 2.2 Operationalization of the information-based resilience index

180 Using this model we generate a very large number of possible trajectories over an information set starting from a historically  
 grounded initial condition (e.g. start of industrial revolution with atm [CO<sub>2</sub>] at 280 ppm). We track the long-run evolution of  
 each trajectory and ask: “Does it reach a SAJOS (safe And just Operating Space (Dearing et al., 2014; Raworth, 2012))”? We  
 extend the approach by Anderies et al. (2023) in not only characterizing the SOS using atm [CO<sub>2</sub>] as the example for  $G$ , but by  
 including a notion of “just” with a per capita income floor per region as a basic proxy. This IBRI thus represents the probability  
 185  $\mathbb{P}$  that the system state at a specified terminal time  $T$ ,  $X(T)$ , is in a set  $\Omega$  deemed to be safe and just, e.g.  $\Omega$  can be defined by



the planetary boundaries  $\cap$  minimum living standards. Then, given the information set  $\mathcal{I}$ :

$$\text{IBRI} = \mathbb{P}(X(T) \in \Omega \mid \mathcal{I}) \quad (6)$$

The information set  $\mathcal{I}$  can, for example, contain information on  $n$  degrees of freedom, the initial condition  $X_0$ , the possible perturbations (e.g. strength of climate damages  $\sigma$  in our model), boundary thresholds ( $G_0$  in our model) or other system parameters in an  $n$ -dimensional object  $\Theta$ .

In our analysis and results we compute the IBRI for two illustrative information cases a) the underlying model structure is perfectly known (no model uncertainty) but some parameters are unknown (parametric uncertainty) and 2) the underlying model structure is not perfectly known, i.e. there is model (structural) uncertainty as well and parametric uncertainty. Therefore, an information set also contains information about the mapping of the state  $X(t)$ , which is encoded by the model  $\mathcal{M}$ . We refer to case a) as the “deterministic many-worlds” (information set  $\mathcal{I}_d = \{\mathcal{M}_d, \dots\}$ ) and case b) as “stochastic many-worlds” (information set  $\mathcal{I}_s = \{\mathcal{M}_s, \dots\}$ ). IBRI is then calculated by integrating (summing and normalizing) over “many-worlds” to determine what proportion of possible World-Earth trajectories reaches the SAJOS (see Fig. 2 for mathematical details).

Of course, our approach works for any uncertainty set, i.e. all parameters are unknown, all equations are stochastic, etc. Our choice of information sets reflects recent sentiments on key uncertainties around the effectiveness of international efforts to decarbonize, support of clean energy, realistic maximum rates of decarbonization, etc. (Lesk et al., 2022; Sinha et al., 2024), Earth system tipping elements (Armstrong McKay et al., 2022; Lenton et al., 2008, 2023), damages due to extreme weather (Newman and Noy, 2023). We therefore choose the decarbonization start point  $T_g$ , the location of the stylized tipping point  $G_0$ , the scaling of climate damages  $\sigma$  and the annual decarbonization rate  $r_e$  as the part of a 4-dimensional hypercube  $\Theta$  that will in small variations be shared for both modeling approaches and that represents the parametric uncertainty. To reduce the dimensionality of this object and thus computation times we chose the parameters to be shared between both regions.

### 3 Results

The elegance of the information-based resilience index (IBRI) is the fact that it incorporates different forms of uncertainty and “subjectivity” in a “rigorous way”. Recall that unless we had a perfect model of the world (“all models are wrong”) and had perfect measurement capabilities, evaluative aspects always enter decision-making processes prominently (“subjectivity”), in particular when answering the question “resilience of what, to what?” (Carpenter et al., 2001). With perfect information, IBRI is either 0 or 1 - trajectories will either reach the SAJOS or not. In the “real world” without perfect information, with limited measurement capacity and irreducible uncertainty due to, e.g., variability and chaotic dynamics,  $0 < \text{IBRI} < 1$ . The beauty of IBRI is that it can be distinct for each actor in the system, based on their information set. Of course it may be the case that many actors converge to the same IBRI as their information sets converge because of high confidence in shared evidence.

We are not suggesting that scientific evidence be disregarded in resilience discussions but, rather, are highlighting the importance of acknowledging epistemic uncertainty and of information as a resource. In fact, IBRI allows us to incorporate epistemic uncertainty with “objective” knowledge. An example might be climate change: it is basically “perfect” knowledge that human



### Calculating the information-based resilience index IBRI

Calculating IBRI involves averaging over the resilience score over a given information set,  $\mathcal{I} = \{\mathcal{M}, \Theta, X_0\}$ , i.e. a collection of models, parameter sets, and initial conditions. For clarity, and without loss of generality, we will illustrate the computation for our case in which  $\mathcal{M}$  and  $X_0$  are fixed so that  $\mathcal{I} = \Theta$ , the hypercube containing all parameter combinations. Let  $\theta_i = \{T_{gi}, G_{0i}, \sigma_i, r_{ei}\} \in \Theta$  (see Table 2). For each  $\theta_i$ , a simulation is run for 610 time steps (1890-2500) and a resilience score,  $R(\theta_i)$  is calculated. In the deterministic case,

$$R_d(\theta_i) = \mathbf{1}_{\{X_i(T;\theta_i, X_0) \in \Omega\}}. \quad (7)$$

For the stochastic case, for each  $\theta_i$ , Monte-Carlo simulations (we set  $N_{sim} = 100$ ) are performed and averaged:

$$R_s(\theta_i) = \frac{1}{N_{sim}} \sum_{j=1}^{N_{sim}} \mathbf{1}_{\{X_{ij}(T;\theta_i, X_0) \in \Omega\}}. \quad (8)$$

Finally, IBRI is calculated by averaging over the samples  $i \in \{1, 2, \dots, N_{samp}\}$ :

$$\text{IBRI}_k(\Theta) = \frac{1}{N_{samp}} \sum_{i=1}^{N_{samp}} R_k(\theta_i \in \Theta), \quad k \in \{d, s\}. \quad (9)$$

IBRI may be easily generalized to the continuous case:

$$\text{IBRI}(\Theta) = \frac{1}{|\Theta|} \int_{\Theta} R(\theta) d\theta, \quad (10)$$

where  $|\Theta|$  is the volume of  $\Theta$ .

**Figure 2.** Mathematical details for calculating IBRI.

emissions cause dangerous change in the climate (IPCC, 2023), but the exact shape of climate futures and human capabilities to steer the climate back to a SAJOS are features of the system that are afflicted with uncertainty. IBRI allows for an honest  
 220 evaluation of resilience in the light of such uncertainties and helps to signify where they need to be reduced for improved decision-making. What matters (for resilience) is that the IBRI is used in a dynamic, iterative (feedback) policy process to steer the WES in a desirable direction.

One important choice that highly impacts the result of a resilience analysis is the boundary of what constitutes a safe and just operating Space. After defining our choice of the SAJOS, we illustrate the capacities of the IBRI with two exemplary  
 225 information sets.

### 3.1 Defining a safe and just operating space

To evaluate whether a trajectory reaches a safe and just operating space,  $\Omega$  must be bounded. We follow Richardson et al. (2023); Rockström et al. (2009) in their definition for the planetary boundaries to set the safe boundary for  $G$  at 350 ppm.

Additionally, we can define a just boundary, for example by assuming that average per capita income  $y = Y/P$  should be  
 230 above roughly \$4000 USD per year for both world regions, which reflects the threshold for being regarded as an upper-middle



**Table 2.** The most relevant parameters for resilience in the model and their ranges for the analysis. Note that these parameters are assumed to be equal for both regions, therefore we omit subscript  $j$ . In the many-worlds case  $G_0$  is either i) distributed in an iso spaced fashion or ii) along a log-normal distribution that is fit to the estimated threshold ranges for the Greenland ice shield. To reduce computational complexity, we assume that both world regions share the same parameters. In the stochastic many-worlds case we additionally vary the type of stochasticity, choosing either gaussian white noise or a jump process reflecting shocks to the economy. Note that the resolution of some of the parameters is reduced in the stochastic case to account for the increase of computational time due to the Monte-Carlo runs with 100 ensemble members.

Parameter	Interpretation	Case 1: Range, Many Worlds	Case 2: Range, Stochastic Many Worlds
$T_g$	Marks the CO <sub>2</sub> concentration at which serious decarbonization efforts begin.	420 – 620, 1 ppm steps	420 – 620, 2.5 ppm steps
$G_0$	CO <sub>2</sub> concentration at which the feedback between CO <sub>2</sub> and uptake switches from negative to positive (tipping point).	i) 420 – 620, 1 ppm steps ii) log-normal distributed	420 – 620, 2.5 ppm steps
$\sigma$	Scaling factor of damages to build infrastructure associated with extreme weather events, in the following referred to simply as climate damages.	1 – 10 % in 1 % steps	2.5 – 10 % in 2.5 % steps
$r_e$	Annual decarbonization rate, e.g. 10 %/year takes the planet to net zero by 2050.	1 – 15 % in 1 % steps	2.5 – 15 % in 2.5 % steps

income economy by the world bank (World Bank, 2025). Such a choice might be justified by the fact that income correlates with increased living standards. Of course, a higher national income does not necessarily come with better living conditions for everyone (Nolan, 2020), in particular if distributed unequally, but within our simplified model we cannot reflect on intra-regional inequalities and have to rely on a reduced measure for the moment. Eventually, for the safe and the just dimension  
 235 alike, it will be crucial to explore the bounds of  $\Omega$  in a way that reflects what is deemed critical for a livable future on the planet. This can mean including, for example, further planetary or social boundaries (Fanning and Raworth, 2025; Richardson et al., 2023; Rockström et al., 2023).

As a last dimension, it is important to choose the time point,  $T$ , at which the condition  $X(T) \in \Omega$  is checked. A strength of this model is its capacity to tractably model relevant basic processes of the World-Earth system that can be expected continue  
 240 to function, at least in a mid-term future. We therefore set  $T = 2500$ . Thus, we have

$$\text{IBRI} = \mathbb{P}(G(T = 2500) < 350 \text{ ppm} \wedge y(T = 2500) > 4000 \text{ USD yr}^{-1} | \mathcal{I}). \quad (11)$$

Figure 3 illustrates a choice of safe and safe and just Operating Spaces (SOS and SAJOS, respectively) that show the three possible attractors of a model trajectory. The shape of a trajectory depends on the 4 parameters from Table 2. These attractors



are: A) A decarbonized, high income world, which coincides with a system range that could be considered safe and just, for  
245 example. C) A certainly unsafe attractor, with a stylized global Earth system tipping point leading to a hothouse Earth state  
with collapse of economic productivity. B) A world in which high climate damages prevent further economic growth while  
at the same time hindering decarbonization, locking civilizations in at medium to high carbon concentrations with decreased  
economic development. Decarbonization is prevented as the initialization-of-decarbonization threshold of atmospheric carbon  
( $T_g$ ) is not reached. Note that the shape of a trajectory before decarbonization ( $T_g, r_e$ ) and before reaching the stylized tipping  
250 point or not ( $G_0$ ) solely depends on  $\sigma$ , which scales climate damages: all ensemble members that share a value of  $\sigma$  share the  
same path before they differ depending on the the other parameters.

Even though a world stuck in such a trajectory might arguably be better off than a world that is heading to attractor C, we  
choose not to count it as “resilient”, due to the inherent myriad of potential dangers in a high-carbon, low-income world (Kemp  
et al., 2022).

### 255 3.2 The deterministic many-worlds information-based resilience index

In this example, we begin with the deterministic standard version of the model, i.e. information set  $\mathcal{I}_d = \{\mathcal{M}_d, \Theta\}$ . Here,  
one world is unambiguously resilient or not, depending on the fulfillment of the resilience condition (see Fig. 2. We create  
our many worlds by varying the parameters shown in Table 2, informed by realistic uncertainty about our world to create  
the 4-dimensional hypercube  $\Theta$  in parameter space. An individual’s many-worlds IBRI is thus defined by their choice of  
260 hypercube. Obviously, this is a subjective choice and can be adjusted accordingly, depending on objectively plausible beliefs  
about plausible socio-economic pathways (similar to the construction of the shared socio-economic pathways; SSPs), which is  
the whole point of the information-based approach.

If we know nothing more about the world than the ranges mentioned above, we can average over the whole space to obtain  
an overall resilience of 0.31. The strength of the information-based resilience index is now that one can imagine all possible  
265 subsets and geometric variations of this parameter space and analyze the overall resilience of the whole object, volumes, areas,  
lines, or points, all reflecting different uncertainties or, put the other way, knowledge about the world. This is illustrated in  
Fig. 4A, which shows the 4-dimensional knowledge landscape projected onto the 2-dimensional space of the decarbonization  
initialization point  $T_g$  versus the location of the stylized tipping threshold  $G_0$ .

Figure 4 is a map of the resilience index IBRI (the conditional probability for reaching the desired state as indicated by  
270 the color bar to the right) to a 2-dimensional  $G_0$ - $T_g$  subspace of the parameter hypercube  $\Theta$ . For each coordinate ( $G_0$ ,  
 $T_g$ ), the model is run for all possible combinations of the remaining 2 parameters knowledge ranges, decarbonization rate  
 $r_e = 0.01, \dots, 0.15$  and climate damage strengths  $\sigma = 0.01, \dots, 0.10$ . IBRI is calculated using Eq. 9 given a particular value of  
 $G_0$  and  $T_g$ . Consider, for example, the point (450, 500): this case would reflect either the assumption or the knowledge that  
decarbonization will begin at 500 ppm, but that the stylized tipping threshold is at 450 ppm. At this point, the resilience index is  
275 0 (dark red color) because when decarbonization begins, the threshold has already been crossed. No matter what combination  
of  $r_e$  and  $\sigma$ , i.e. no matter how low climate damages and how high decarbonization rates, no trajectory will end up in a safe  
and just space and the resilience index is 0. The resilience index is indeed 0 for all  $G_0$ - $T_g$  combinations in the dark red region.

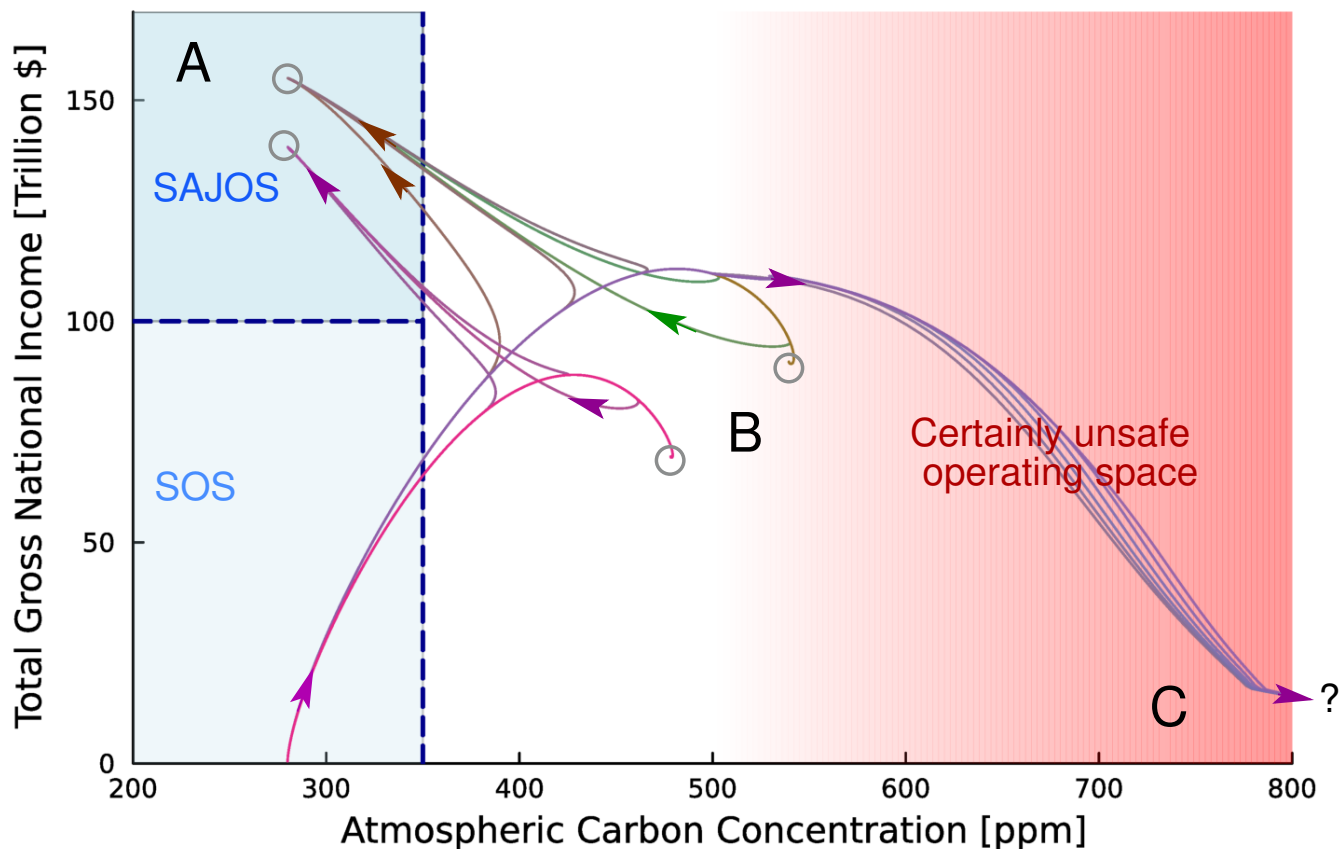


**Figure 3.** Evaluative choices of safe and safe and just operating spaces for the World-Earth model used in this study. Trajectories combine a range of values for decarbonization time point  $T_g$  (from 380 to 700 ppm), stylized tipping threshold  $G_0$  (500 or 1000 ppm), climate damage  $\sigma$  (2.5 % or 7.5 %) and decarbonization rate  $r_e$  (10 %). The trajectories showcase the three attractor ranges (A, B, C) of the model. Gray circles indicate long run equilibria, i.e.  $X(T)$  for large  $T$ . Arrows indicate direction of motion for various trajectories for different  $\theta_i$ .

Analogously, the resilience index is 1 for all  $G_0$ - $T_g$  combinations in the dark blue region because decarbonization begins well before the stylized tipping threshold so uncertainty in other parameters does not matter.

280 The narrow white diagonal region indicates the combinations of  $G_0$  and  $T_g$  for which the resilience index is roughly 0.5. For these values roughly half of the trajectories reach the desired state as  $r_e$  and  $\sigma$  are varied. As we move up and to the left, decarbonization occurs progressively later relative to the threshold and, as we would expect, the resilience index decreases rapidly and fewer trajectories reach the desired state. As we move down and to the right, decarbonization occurs progressively earlier relative to the stylized tipping threshold and the number of trajectories reaching the desired state increases.

285 Based on this analysis, the  $G_0$ - $T_g$  state space can be divided into three regions: a mostly (non-)resilient space shown in dark blue (red) in which decarbonization occurs so early (late) that information about parameters is not important and the system is

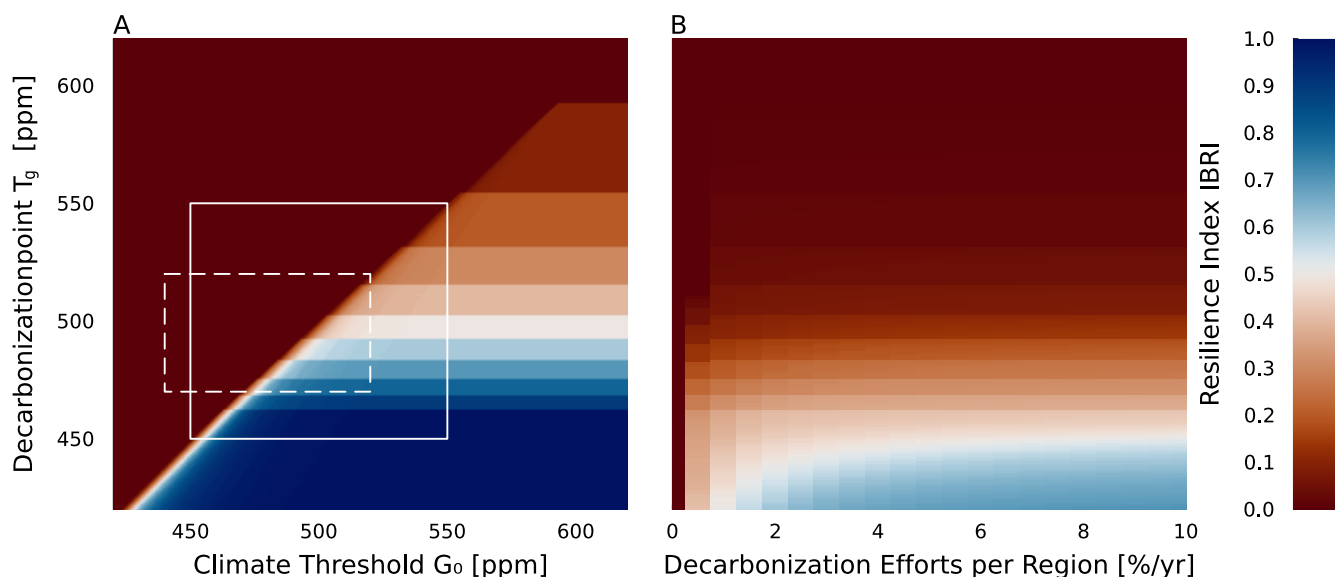


**Figure 4.** Panel A: The information-based resilience index, i.e. the conditional probability of a simulation run to end up in the desired state, mapped onto the parameter space of the decarbonization Point  $T_g$  and the stylized tipping threshold  $G_0$  ( $\sim 10^6$  ensemble members). Each pixel shows the average resilience index over fixed  $T_g$  and  $G_0$ , summing over all combinations of decarbonization rate  $r_e$  and climate damage strengths  $\sigma$ . For example, at  $G_0 = 450$  ppm and  $T_g = 500$  ppm, meaning that decarbonization is only started after the threshold has been crossed, none of the simulations ends up in the desired state, no matter which of the possible decarbonization rates or climate damage strengths. Therefore, the resilience index is 0. Some different possible information scenarios indicated, for example, by the rectangles R1 (solid) and R2 (dashed) and their respective resilience indexes are indicated in Table 3. Panel B: IBRI map over  $(r_{e1} + r_{e2})$ - $T_g$  space with the distribution of  $G_0$  informed by data from the Greenland ice sheet ( $\sim 10^6$  ensemble members). See Table 3 for resilience values.

completely resilient or perfectly non-resilient. These zones are divided by an intermediate zone around the white diagonal line where information about  $r_e$  and  $\sigma$  becomes important.

The location of this boundary region shows that because of inertia in the model, decarbonization has to start some 20-30 ppm  
 290 before the threshold is reached. This is what we call critical delay, which could be interpreted as a reaction time to start the decarbonization. The sharpness of this shift is determined by the ranges of the decarbonization rates and the parametrization of climate damages, i.e. the more options there are the smoother the transition becomes. Thus, in a setting close to where  $T_g$  and  $G_0$  are separated by this critical delay,  $r_e$  and  $\sigma$  become very important in determining whether the WES is resilient or not. As  $T_g$  and  $r_e$  are arguably the only two parameters that a World system might influence, the most effective way to design a  
 295 resilient WES, rather unsurprisingly, is therefore decarbonising early enough before the threshold. The more nuanced insights from the analysis occur near the threshold region which, given historical response to climate change, are the most relevant (it seems unlikely that nation states will agree to decarbonise early).

One important nuance is the occurrence of step-like gradients in the resilient (blue) regime below the diagonal regime shift in which full resilience is not reached everywhere, even though decarbonization would start early enough in most cases.



300 This originates from the hidden dimensions encoded by parameters of climate damage strength  $\sigma$  and decarbonization rates. In particular, where climate damages  $\sigma$  are high, trajectories can get stuck in a low economic output world (attractor B in Fig. 3), which prevents them from returning to a safe and just operating space. The frequency of occurrence of these worlds depends on the possible values of  $\sigma$ . The resolution of 10 possible values of  $\sigma$ , which is constrained by computational costs, is thus reflected in the 10 visible steps. For very high values of  $T_g$  the starting point of decarbonization occurs at very high  
305 atmospheric carbon concentrations and is never reached, as even very low climate damage rates are at some point strong enough to suppress economic growth and thus emissions that would otherwise trigger the decarbonization. Lowering  $T_g$  (moving down the heatmap) at some point the set of trajectories with the lowest climate damages (that all follow the same path before  $T_g$  or  $G_0$ ) touches the decarbonization threshold and all of them are enabled to return to the safe attractor, as  $G_0$  is high enough in this region. For lowering  $T_g$  further, the next higher set of trajectories with a shared  $\sigma$  is reached and so on, until  $T_g$  is low  
310 enough such that even high damage trajectories with a very bent curve are able to reach decarbonization and all sets reach the safe attractor. The 10 values of  $\sigma$  with a possible safe or unsafe (true, false) outcome thus yield the 11 regions of different resilience below the diagonal, according to combinatorics.

IBRI can also be used to explore different information (sub)sets, by either redefining the original parameter hypercube, or only considering part of it:  $\Theta'$ . This yields a new information set  $\mathcal{I}'_d = \{\mathcal{M}_d, \Theta'\}$ . For example, if we believe that the threshold  
315 lies between 450 and 550 ppm and that decarbonization will possibly start between 450 and 550 ppm, we can integrate over the area in the rectangle R1 and obtain an overall resilience of 0.32, slightly increasing from the overall resilience for the original parameter range. If even more information is obtained, such that  $T_g = [470, 520]$  and  $G_0 = [440, 520]$ , i.e. it becomes certain that decarbonization will start a bit later overall and the stylized tipping threshold is closer, integrating over R2 produces an  
320 IBRI of only 0.17. Therefore, depending on the knowledge (and given appropriate action if knowledge is available) about the system, the resilience can change. This is the essence of the information-based resilience index. With learning more about the system and thus reducing uncertainties, you could learn that you are more or less resilient. Such changes in resilience are critical inputs in a dynamic policy process.

### 3.3 Refining the information set with Earth system resilience knowledge

In Fig. 4B, a resilience index landscape is shown again, as governed by the two parameters that can possibly be controlled by  
325 the World system as means to adapt,  $T_g$  and total combined decarbonization rates ( $re_1 + re_2$ ). Those parameters were shown before to be crucial to overall resilience. Now the stylized tipping threshold is not distributed uniformly but, rather, along a log-normal distribution motivated by a threshold range of a typical tipping element. Here, we take the Greenland ice shield as an example for several tipping elements at risk to be triggered by projected global warming projections (Armstrong McKay et al., 2022; Robinson et al., 2012). The 5 % quantile of the distribution is chosen such that it coincides with the lowest estimated  
330 possible temperature threshold for Greenland ice sheet tipping, 0.8 °C, and the 95 % quantile to match the highest, 3.0 °C. For this, ppm is converted to temperature using a rough rule-of-thumb linear approximation, where an increase of 100 ppm equals 1 °C temperature change, as our model does not include a more sophisticated representation of climate. The other parameters remain the same as in Table 2 ii).



**Table 3.** The results of the information-based resilience assessment depending on the chosen information subset, i.e. the modelling choices and parameter uncertainty ranges included within the assessment.

Information Set	Parameter Uncertainty	IBRI
$G_0$ Gridded	Whole object	0.31
	R1	0.32
	R2	0.17
$G_0$ Informed by Greenland Ice Sheet	Whole object	0.21
	5% decarbonization rate	0.18

With this newly informed threshold, overall resilience of all parameter ranges is 0.21. In this case, it becomes even clearer that the relevant parameter to improve resilience is the start time of decarbonization, as even an increase of decarbonization rates to very high and seldomly observed values ( $>8$ - $10$  %/yr per region) increases resilience only marginally if decarbonization starts too late. If one considers an annual per region decarbonization rate of 5 % (which can already be considered high, keeping in mind that emissions are still rising in parts of the world), resilience decreases even further to 0.18. This tells a grim story of the likelihood to reach a desired operating space with the presence of a possible stylized tipping threshold informed by estimates of the Greenland ice sheet tipping range. Of course, a range of modeling decisions play a role here, such as the assumed log-normal shape for the distribution of possible threshold locations, but this further emphasizes the importance of reducing knowledge gaps for crucial boundary elements of the Earth system in resilience analysis. In general, this shows that knowledge about the functioning and resilience (represented by the threshold here) of the Earth system is central to constrain our information-based approach. Table 3 summarizes the IBRI values for each of the cases discussed so far.

### 3.4 Modeling stochasticity in the World–Earth system

After having laid out how an information-based resilience assessment works with the deterministic many-worlds model in two cases, we further showcase its applicability and comparability for different variations of the original model. We therefore include multiple model representations in the set of models for the stochastic information set  $\mathcal{M}_f$ . For this, in particular, we allow for stochastic variation of two kinds (a Wiener process and a Ornstein-Uhlenbeck process with Poisson jumps) in the model and compare the resulting implications on resilience. Additionally, we implement a possible variation of the Earth system where crossing the stylized tipping threshold  $G_0$  does not lead to a hothouse runaway climate, but to a loss of buffering capacities of the Earth system sinks, i.e. the carbon uptake rate by the Earth system  $u$  in Eq. 3 is set to zero,  $u = 0$ , after crossing the threshold  $G_0$  instead of an additional release of carbon. This leads to a strong drifting of the Earth system, similar to the trajectories that reached attractor B of Fig. 3 before, but reaching deeper into a high carbon, high damage world. We include this variant to showcase how our model can be extended to answer related resilience questions, i.e. what if the Earth system lost its supporting buffering capacities.

In the first stochastic variant, we apply a multiplicative Wiener process for the capital fluxes  $K_j$  and the emission intensity  $e_j$  in both regions ( $j = 1, 2$ ), such that from Eq. 3 and Eq. 5 we obtain a stochastic differential equation with classical Brownian



motion of the form

$$360 \quad dK_j = (I_j - \delta_j K_j - \sigma S(G) K_j) dt + \varsigma K_j dW_{K_j}(t), \quad (12)$$

$$de_j = (-z r_e e_j) dt + \varsigma e_j dW_{e_j}(t), \quad (13)$$

where  $\varsigma$  describes the scaling of the multiplicative noise, in our analysis either 2.5 % (“small”) or 7.5 % (“large”), to the current state  $K_j(t)$ . Thus, additionally to the continuous climate damages introduced by  $\sigma S(G)$ , there can now be processes that mimic annual random shocks to the economy. The same is done for the decarbonization rate, allowing for stochastic variation also to the resulting level of  $G$ . Both capital fluxes and emissions are inherently fluctuating properties in the real world. For both, we assume the fluctuations to be proportional to their current level, leading to the representation via multiplicative noise.

Figure 5 showcases the changed dynamics of the model for a set of representative trajectories and each type of stochasticity, as well as Earth system response. Figure 5B shows how the trajectories of the continuous stochastic system (for a small 2.5 % scaling of the noise) have increased variability, but still follow the overall attractors that are found for the deterministic system, shown in Fig. 5A. We choose one parameter set for a favorable (no stylized tipping threshold), a drifting (to loss of sinks for crossing of threshold) and a critical (runaway hothouse climate for crossing of threshold) Earth system, where  $T_g = 500$  ppm,  $\sigma = 3$  % and  $r_e = 10$  %. In the second stochastic variant, we implement shocks to the total factor productivity  $A_j$ .

For this, we implement  $A_j$  as two new state variables that follow a classic relaxation process (Ornstein-Uhlenbeck without noise):

$$375 \quad A_j = \gamma_i (A_{0,j} - A_j), \quad (14)$$

where  $\gamma_j = 0.1$  is the relaxation rate equal for both regions and  $A_{0,1} = 2.7$  and  $A_{0,2} = 1.7$  are the maximum total factor productivities for both regions. We then define Poisson jumps  $dN_j(t)$  that afflict  $A_j(t)$  with rates  $\lambda$  depending on the current state of the externality (i.e. the higher the  $G$ , the more often a climate shock affects the economy):

$$\lambda_j(G) = \frac{\lambda_0}{1 + \exp[-k(G - G_p)]}, \quad (15)$$

380 where  $\lambda_0 = 0.05$  and  $k = 1$  are scaling factors and  $G_p = 300$  ppm gives the minimum externality for a shock to occur. When a shock occurs, it randomly gets assigned a shock size  $\xi_i$  of 0 - 20 % of the current level:

$$A_j \mapsto A_j - \xi_i A_j, \quad \xi_i \sim \text{DiscreteUniform}(0, 0.2), \quad (16)$$

yielding the final stochastic SDE:

$$dA_j = \gamma_j (A_{0,j} - A_j) dt - \xi_j A_j dN_j(t). \quad (17)$$

385 With this, we obtain trajectories with larger jumps rather than continued variability, as can be seen in Fig. 5C. Both cases of stochasticity are a way to include dynamic uncertainty on how the World system in particular will react to opposing pressures. In principle one could use one or an overlay of both types of the model to include negative impacts like societal unrest or positive improvements, for example technological progress.

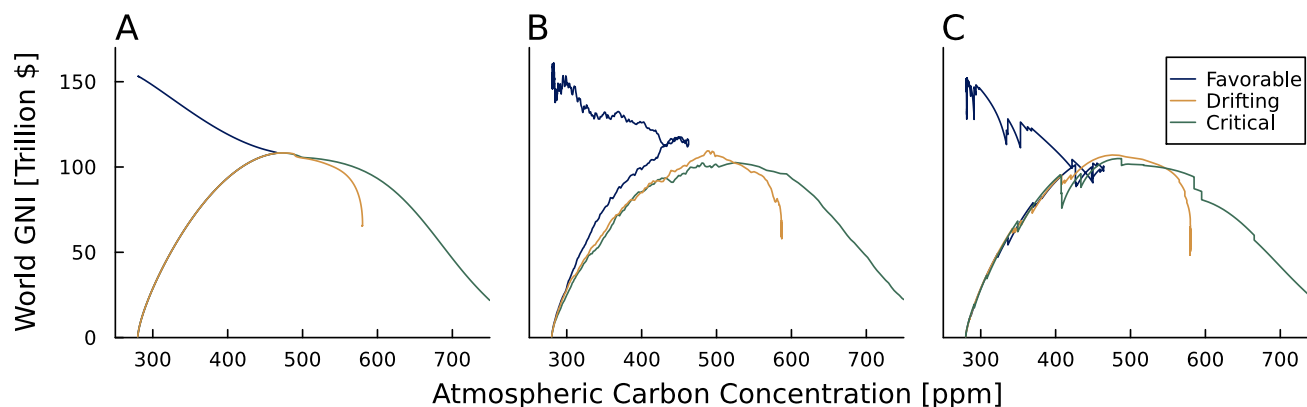


**Figure 5.** Comparative trajectories total world income vs. atmospheric carbon for A) the deterministic standard model, B) a stochastic model with continuous variation in  $K$  and  $re$  (for 2.5 % variation) and C) a stochastic model with a jump process reflecting sudden losses in total factor productivity. Additionally, three types of Earth system response are depicted: a) favorable, i.e. the threshold is not crossed, b) drifting, the threshold is crossed and the Earth system response is a complete loss of buffering capacities and c) critical, the threshold is crossed and the response is an additional release of carbon.

### 3.5 The stochastic many-worlds information-based resilience index

390 We repeat our resilience analysis for all three cases (deterministic, shocks and two Wiener process cases with different scalings of noise) with the reduced parameter ranges from Table 2 (also applied to the deterministic version, to ensure comparability) to account for increased computation times in the stochastic cases due to the Monte Carlo analysis with  $N_{samp} = 100$  ensemble members. In the way that our resilience conditions are set right now, the drifting Earth system case does not make a qualitative difference, since crossing the threshold in all cases does not meet the safe and just operating space requirements. We therefore  
395 use the standard runaway model for crossing for these calculations. Note that this system can still lead to “drifting” trajectories, as defined as attractor B in Fig. 3, that eventually get stuck at the very point in which climate damages equal any surplus for investment, freezing the system in the current state of carbon concentration  $G$ , and total economic output  $Y$ . In future analyses with refined resilience conditions the real drifting Earth system case might be of great relevance though, and was introduced before for illustrative purposes.

400 The resilience assessment of all four cases is as follows: The IBRI for the deterministic, shock stochastic, continuous stochastic with small (2.5 %) variation and continuous stochastic with large (7.5 %) variation models are 0.29, 0.28, 0.31 and 0.50, respectively. It can be seen that the deterministic and the shock case yield similar outcomes, with the shock case being slightly less information-based resilient overall. This is due to the fact that shocks only affect the economic dimension of the model, without significantly altering the qualitative shape of trajectories: while shocks can lead to significantly different trajectories  
405 on the micro level (size and frequency of shocks), the overall statistic probability to reach a desired state does not change under our assumptions, as the economy cannot “break”.



This is confirmed by comparing Fig. 6 A and B, which show the 2-dimensional projection of the resilience space onto  $T_g$  and  $G_0$  for the reduced information sets for the deterministic and the shock case. The only difference is found in the transition between the steps that are introduced by  $\sigma$  (now reduced to four possible values): the transitions to the next less resilient subspace happen at slightly smaller values of  $T_g$ , while also becoming smoother. This is due to the probability of a shock affecting a trajectory shortly before reaching  $T_g$ , trapping the system (temporarily) in the high-carbon, low-income attractor. For this, a large shock to the economy is needed, which shortly brings the economy into a backdrop state, allowing the Earth system to take up carbon, reducing continuous climate damages, allowing the economy to grow again. In the meantime, as the economy has not fully recovered again, another (ever smaller) shock is likely to send it on the same detour again, diminishing but not eliminating the possibility to escape the limit cycle. This attractor is related to attractor B found in Fig. 3 and only found in conditions where climate damages already suppress growth enough, such that additional damage (here via the shocks) can stop development before reaching  $T_g$  and thus getting the trajectory stuck. The probability of such a shock increases quickly the closer  $T_g$  comes to the transition level for the corresponding value of  $\sigma$ , as the aforementioned condition is fulfilled and more time is spent close to the attractor, allowing badly timed shocks to send a trajectory into such a cycle. This reduces and smoothens out the transitions, eventually slightly decreasing the overall information-based resilience index.

In reality, a society would deeply care if it is on a rather smooth or bumpy trajectory, as World–Earth resilience also depends on the capacity of the World system to recover from economic shocks. In future models such a feedback loop between World system shocks and adaptive capacities will be a crucial extension to the model.

The continuous stochastic cases on the other hand do show (slightly) increased resilience and also qualitatively a different picture when looking on their resilience heat maps, as shown in Fig. 7C and D. This is due to the fact that the continuous stochasticity does affect economic processes as well as Earth system relevant processes here. The dynamic uncertainty within the decarbonization process has a twofold effect.

First, trajectories that would have gotten stuck in a high-climate-damage, low-economic output world (attractor B from Fig. 3), now do not get stuck, as stochastic variation allows them to escape the small basin of attraction, which damages exactly equal investment potential. Therefore the grades that were present in the deterministic and shock-stochastic model now get resolved to a more smooth transition spanning the whole (possibly) resilient regime below the diagonal. This transition mainly depends on the decarbonization time point as well as on values of  $\sigma$ . Now, later decarbonization and higher climate damage levels bring the system further away from the safe and just operating space, by allowing larger detours into the high-carbon, low-economic-output world. This costs trajectories substantially more time, as the World system has to recover this on the way back to the safe and just operating space, making the time constraint for the safe and just operating space, i.e. reaching it by 2500, relevant in this case. Thus, some trajectories that are headed towards the safe and just operating space are still considered non-resilient, leading to the smooth transition in the direction of  $T_g$ .

Second, for high values of stochasticity, some trajectories of an ensemble for the same parameter choice that otherwise would cross a threshold  $G_0$ , will not cross it because of fluctuations in the decarbonization speed. This is due to the variation an uncertainty in the resulting atmospheric carbon levels  $G$ .

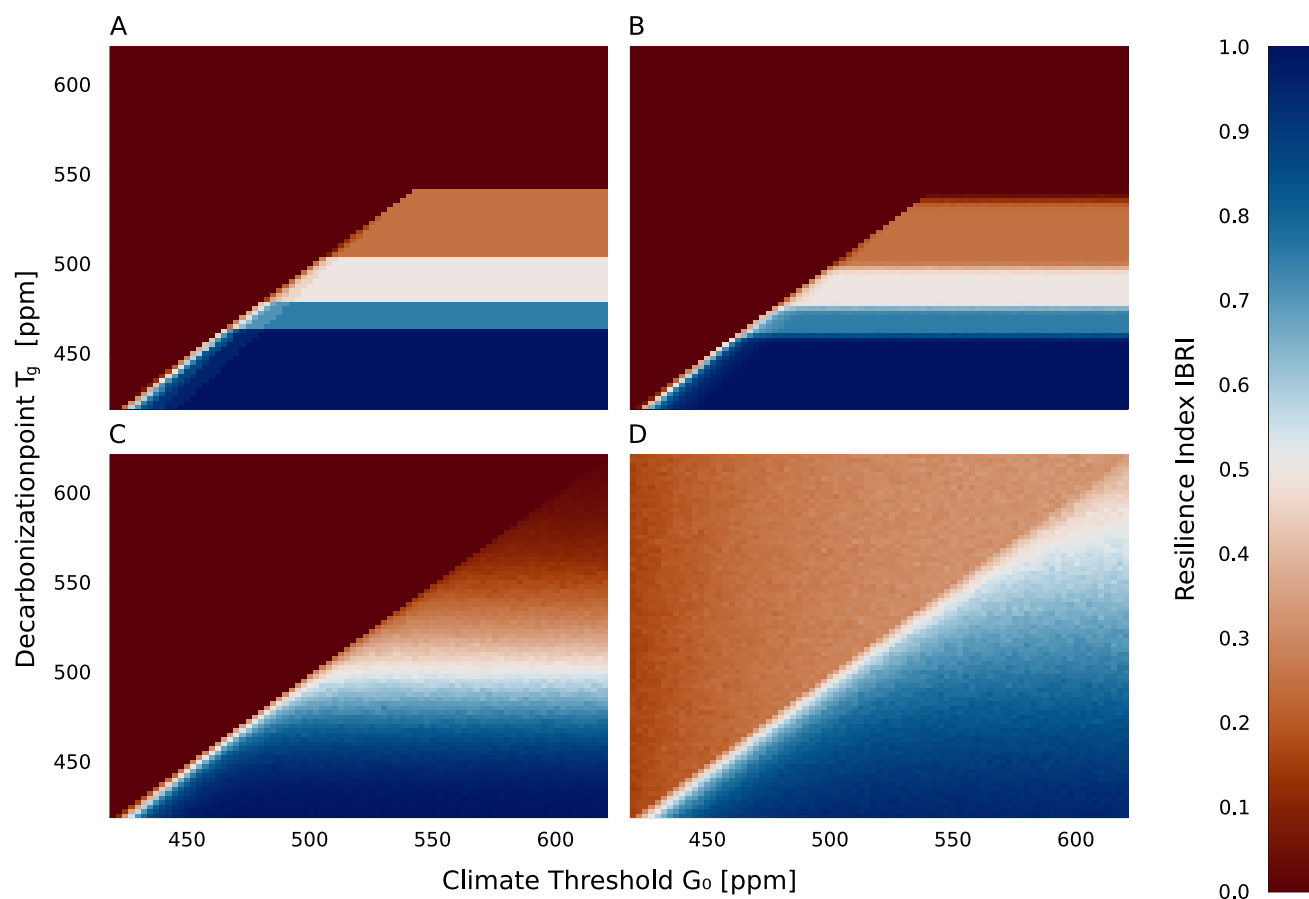


**Figure 6.** The information-based resilience index map for A) the deterministic model (note the reduced resolution to account for increased computational cost due to ensemble runs), B) the model with shocks to the total factor productivity and C) the model with stochastic variation in the form of a Wiener process, applied to the capital fluxes and the decarbonization rates and scaled to 2.5 % variation from the current state, or D) 7.5 %. (All:  $\sim 10^6$  ensemble members).



For even larger noise, the resilience thus rises to 0.50. This is surprising, as one would assume the expectation value of trajectories that cross or do not cross the threshold because of noise to be the same, because of the symmetry of the single noise processes. This result can be explained when looking at the model dynamics again: While the noise process in the decarbonization equation itself is symmetric, the decarbonization itself is a process that is asymmetric: in the domain that is more resilient in the deterministic case, the threshold is far enough away such that the economy can be turned around before crossing it in most cases, even for small decarbonization rates. If such a stochastic process reduces these rates temporarily, it does not reduce the chance to reach the desired state by as much, therefore mostly leaving this domain untouched. In particular, since the decarbonization by default is never negative, i.e. the worst that can happen is a very slow decarbonization, not a re-carbonization. In the domain that was already mostly non-resilient before, a decreased decarbonization rate can thus only marginally decrease resilience, while a highly increased decarbonization rate can actually buffer the trajectory enough from reaching the threshold and thus only positively affecting the overall resilience. This can only be achieved because of highly increased decarbonization efforts due to the dependency of the Brownian motion on the current state, which introduces a form of path dependency. These increased decarbonization efforts reach values around 2 times the size of the maximum decarbonization rate of  $r_e = 15\%$  that we allow for (which is already quite high). This path-dependent decarbonization is hence only possible for a highly adapting world system in which decarbonization can be evermore ramped up, exploiting previous achievements. In a realistic world, where decarbonization rates are not likely to exceed a certain upper ceiling, this increase in resilience is not really reachable. Also here, sufficiently early and speedy decarbonization remains the main tool to achieve a more resilient world.

The difference in overall resilience between the cases with different types of stochasticity and noise showcases the power of the information-based resilience approach again. One could not only ask the question of how resilience changes with different knowledge about “parameters” of our world, but also how resilience changes with ranges of noises or shocks that one deems possible. The overall resilience of a world which could have the above described stochasticity is thus the mean of both these possible worlds, 0.295. This softens the question of “Resilience of what to what”, by allowing the “to what” to possibly have different ranges and impacts and thus puts the focus on the evaluative, epistemically grounded choice of the “of what”. Similarly, one could compare scenarios with different relevant processes present or not, for example one extends the analysis of one tipping element by allowing for multiple interacting tipping elements, and assess the likelihood/risk of tipping cascades (Wunderling et al., 2023). In the same modeling framework one can then analyze how the presence of interactions between tipping elements decreases (or, less likely given the current state of literature (Wunderling et al., 2024), increases) the overall resilience. This comparability is what makes the information-based resilience understanding so highly operational.

#### 470 4 Conclusions

This work has presented an information-based approach to formalizing resilience and operationalized it using a World-Earth system model. Our goal has been to develop an understandable, policy-relevant measure that can feed into real-world policy processes. Our study is motivated by the need to move beyond theory-based metrics and vague notions of resilience that are



of limited value in practice. Understanding resilience through an information-based lens highlights the important fact that  
475 in collaborative decision-making there is a negotiation of beliefs. IBRI provides a vehicle for scientists, citizens, and policy  
actors to think and communicate about their beliefs and assumptions from the start, consistent with recent calls for relational  
approaches to simulation modeling (Klein et al., 2024). Each actor has their own beliefs and IBRI. Some groups with shared  
beliefs will share very similar IBRI (but perhaps for different reasons), and differences across groups may be large. The key is  
that IBRI provides a currency for negotiating toward collective decisions.

480 Beyond its virtue as a mechanism to help reconcile and bound different beliefs about WES functioning and potential futures,  
IBRI may also help dislodge attention from the “right” model or “better data”. IBRI is model agnostic, i.e. it can be calculated  
over any general information set  $\mathcal{I} = \{\mathcal{M}, \Theta, X_0\}$  including a range of models using the simple method summarized in Fig.  
2. In particular, it allows for the assessment of future choices given today’s beliefs. Most importantly, IBRI can help identify  
the most contested and impactful uncertainties that need to be reduced with urgency. While we fully appreciate that the IPCC  
485 process and model comparison activity are similar in spirit, the outputs, e.g. time trajectories with uncertainty envelopes is  
less intuitive and less readily communicable than a single conditional probability. Further, and perhaps most importantly,  
IBRI strongly discourages thinking about resilience in absolute terms because as we have discussed, without uncertainty (i.e.  
subjectivity in some form), resilience is either zero or one. What is important is relative uncertainty. How is resilience changing  
over time as our understanding of the world changes? It is this change in resilience that is a useful policy tool in driving  
490 decision-making. Additionally, focusing on a change- and solution-based measure instead of a state- and problem-based one  
might be related to a higher motivation to act in general (Said and Wöflf, 2025). In the illustrative model presented here,  
this takes the form of investments in learning more about the location of tipping elements through efforts such as the Global  
Tipping Points Report and systematic model intercomparison projects like TIPMIP (Lenton et al., 2025; Winkelmann et al.,  
2025) or analysis of admissible emission pathways (Bossy et al., 2025; Schleussner et al., 2022). In particular, knowledge  
495 about the resilience of the Earth system was shown to be crucial to constrain IBRI. Measures of stochastic and topological  
resilience and IBRI interact and depend on each other. Operationalizing IBRI in this way will focus attention on the challenging  
problem of defining information sets that reflect initial beliefs about the system that will propagate through the assessment.  
Deep uncertainties and unknown unknowns form another obstacle. In future work, we plan to analyze how IBRI impacts the  
dynamics of the World-Earth system when endogenized in a fully coupled decision-making loop .

500 One potential risk of IBRI is proxy failure (John et al., 2024). That is, when a measure (IBRI) becomes a target, it ceases to  
be a good measure, according to Goodhart’s formulation. For example, when trying to maximize an IBRI, a policymaker could  
update their beliefs and end up with less accurate information about the system than is available. If one does not believe in  
climate change-induced damages, one would rate the system as perfectly resilient. Ignorance can improve resilience. The risk  
of proxy failure here is not that all IBRI optimizing policy makers would suddenly become climate-change deniers. The history  
505 of proxy failure cases has shown that the mechanisms by which the proxy fails are more subtle, hard to predict, and in some  
cases, have disastrous consequences. Having said that, the fact that all stakeholders may have different IBRI that enter into  
collective decision-making in which beliefs are negotiated may reduce the potential for proxy failure. Of course, as always, it  
is the nature of institutional arrangements that structure collective action that is the key determinant of the value of any index.



In the right institutional context, with an iterative decision-making process that emphasizes changes in the resilience index and  
510 deliberation around uncertainty rather than the “right measure”, IBRI may be a powerful tool for better decision-making.

In the future, it will be crucial to extend our information-based resilience assessment to, first, a more detailed representation  
of bio-geophysical aspects of the Earth system, which is currently showing worrying signs of a resilience loss (Ripple et al.,  
2024), and, second, to assess new lines of coupled, co-evolving World-Earth system models that are capable of reflecting  
uncertainties within the World-, the Earth-, but most importantly the feedback interactions within the World-Earth system  
515 model. A possible extension to the stochastic model presented here is a feedback loop between shocks that cascade from the  
Earth system to the World system, affecting its adaptive capacities.

*Code and data availability.* The code of our model is published on Zenodo <https://doi.org/10.5281/zenodo.17100929> and available on  
GitHub <https://github.com/zugnachpankow/An-Information-Based-World-Earth-System-Resilience-Index>. Corresponding data that can be  
used to reproduce our results is published and available on Zenodo <https://doi.org/10.5281/zenodo.17098743>.

520 *Author contributions.* J.M.A., M.B. and J.F.D. have conceived and designed the study. J.M.A. has lead the conceptual design of the model,  
including the first simulation model implementation. M.B., I.F., N.W. and J.F.D. have contributed to the conceptual design. M.B. has led  
the further development and performance improvement of the model and has performed model simulations. J.M.A. and M.B. have led the  
writing of the manuscript. J.M.A. has visualised the model description. M.B. visualised simulation results. All authors contributed to the  
writing of the manuscript and the discussion of results. J.F.D.,and J.R. have supervised and acquired financial support for the study. J.M.A.  
525 and M.B. share the lead authorship.

*Competing interests.* J.F.D. is member of the editorial board of Earth System Dynamics. J.F.D. serves as editor for the special issue to which  
this paper belongs. The authors declare no further competing interests.

*Acknowledgements.* M.B., J.M.A., J.F.D., N.W., and J.R. acknowledge support from the European Research Council Advanced Grant project  
ERA (Earth Resilience in the Anthropocene, ERC-2016-ADG-743080).

530 J.F.D. acknowledges financial support from the European Union’s Horizon 2.5 - Climate Energy and Mobility programme under grant  
agreement No 101081661 (project WorldTrans) and the project “CZS Research Groups for Earth System Modelling” funded by the Carl-  
Zeiss-Stiftung.

J.F.D. and J.R. acknowledge financial support by the Generation Foundation, the Global Challenges Foundation, and Partners for a New  
Economy via the Earth4all project.

535 The authors gratefully acknowledge the European Regional Development Fund (ERDF), the BMBF and the Land Brandenburg for sup-  
porting this project by providing resources on the high-performance computer system at the Potsdam Institute for Climate Impact Research  
(PIK).

<https://doi.org/10.5194/egusphere-2025-6345>  
Preprint. Discussion started: 11 February 2026  
© Author(s) 2026. CC BY 4.0 License.



The authors further acknowledge the support of Ricarda Winkelmann during the study.  
AI tools have been used for spelling and grammar checks.



## 540 References

- Anderies, J. M., Janssen, M. A., and Walker, B. H.: Grazing Management, Resilience, and the Dynamics of a Fire-driven Rangeland System, *Ecosystems*, 5, 23–44, <https://doi.org/10.1007/s10021-001-0053-9>, 2002.
- Anderies, J. M., Carpenter, S. R., Steffen, W., and Rockström, J.: The topology of non-linear global carbon dynamics: from tipping points to planetary boundaries, *Environmental Research Letters*, 8, 044 048, <https://doi.org/10.1088/1748-9326/8/4/044048>, publisher: IOP Publishing, 2013a.
- 545 Anderies, J. M., Folke, C., Walker, B., and Ostrom, E.: Aligning Key Concepts for Global Change Policy: Robustness, Resilience, and Sustainability, *Ecology and Society*, 18, art8, <https://doi.org/10.5751/ES-05178-180208>, 2013b.
- Anderies, J. M., Barfuss, W., Donges, J. F., Fetzer, I., Heitzig, J., and Rockström, J.: A modeling framework for World-Earth system resilience: exploring social inequality and Earth system tipping points, *Environmental Research Letters*, 18, 095 001, <https://doi.org/10.1088/1748-9326/ace91d>, 2023.
- 550 Armstrong McKay, D. I., Staal, A., Abrams, J. F., Winkelmann, R., Sakschewski, B., Loriani, S., Fetzer, I., Cornell, S. E., Rockström, J., and Lenton, T. M.: Exceeding 1.5°C global warming could trigger multiple climate tipping points, *Science*, 377, eabn7950, <https://doi.org/10.1126/science.abn7950>, 2022.
- Baird, J., Blythe, J. L., Murgu, C., and Plummer, R.: A scoping review of how the seven principles for building social-ecological resilience have been operationalized, *Ecology and Society*, 29, <https://doi.org/10.5751/ES-15114-290220>, publisher: The Resilience Alliance, 2024.
- Barfuss, W., Donges, J. F., Lade, S. J., and Kurths, J.: When optimization for governing human-environment tipping elements is neither sustainable nor safe, *Nature Communications*, 9, 2354, <https://doi.org/10.1038/s41467-018-04738-z>, publisher: Nature Publishing Group, 2018.
- Beckage, B., Gross, L. J., Lacasse, K., Carr, E., Metcalf, S. S., Winter, J. M., Howe, P. D., Fefferman, N., Franck, T., Zia, A., Kinzig, A., and Hoffman, F. M.: Linking models of human behaviour and climate alters projected climate change, *Nature Climate Change*, 8, 79–84, <https://doi.org/10.1038/s41558-017-0031-7>, publisher: Nature Publishing Group, 2018.
- Berkes, F. and Ross, H.: Community Resilience: Toward an Integrated Approach, *Society & Natural Resources*, 26, 5–20, <https://doi.org/10.1080/08941920.2012.736605>, 2013.
- Bossy, T., Ciais, P., Tanaka, K., Lecocq, F., Bousquet, P., and Gasser, T.: Spaces of anthropogenic CO<sub>2</sub> emissions compatible with climate boundaries, *Nature Climate Change*, 15, 1307–1314, <https://doi.org/10.1038/s41558-025-02460-5>, publisher: Nature Publishing Group, 2025.
- Brown, K. and Westaway, E.: Agency, Capacity, and Resilience to Environmental Change: Lessons from Human Development, Well-Being, and Disasters, *Annual Review of Environment and Resources*, 36, 321–342, <https://doi.org/10.1146/annurev-environ-052610-092905>, 2011.
- 570 Carpenter, S., Walker, B., Anderies, J. M., and Abel, N.: From Metaphor to Measurement: Resilience of What to What?, *Ecosystems*, 4, 765–781, <https://doi.org/10.1007/s10021-001-0045-9>, 2001.
- Carpenter, S. R. and Cottingham, K. L.: Resilience and Restoration of Lakes, *Conservation Ecology*, 1, <https://www.jstor.org/stable/26271648>, publisher: Resilience Alliance Inc., 1997.
- Crutzen, P. J.: Geology of mankind, *Nature*, 415, 23–23, <https://doi.org/10.1038/415023a>, publisher: Nature Publishing Group, 2002.
- 575 Dearing, J. A., Wang, R., Zhang, K., Dyke, J. G., Haberl, H., Hossain, M. S., Langdon, P. G., Lenton, T. M., Raworth, K., Brown, S., Carstensen, J., Cole, M. J., Cornell, S. E., Dawson, T. P., Doncaster, C. P., Eigenbrod, F., Flörke, M., Jeffers, E., Mackay, A. W., Nykvist,



- B., and Poppy, G. M.: Safe and just operating spaces for regional social-ecological systems, *Global Environmental Change*, 28, 227–238, <https://doi.org/10.1016/j.gloenvcha.2014.06.012>, 2014.
- Donges, J. F. and Barfuss, W.: From Math to Metaphors and Back Again: Social-Ecological Resilience from a Multi-Agent-Environment Perspective, *GAIA - Ecological Perspectives for Science and Society*, 26, 182–190, <https://doi.org/10.14512/gaia.26.S1.5>, 2017.
- 580 Donges, J. F., Winkelmann, R., Lucht, W., Cornell, S. E., Dyke, J. G., Rockström, J., Heitzig, J., and Schellnhuber, H. J.: Closing the loop: Reconnecting human dynamics to Earth System science, *The Anthropocene Review*, 4, 151–157, <https://doi.org/10.1177/2053019617725537>, publisher: SAGE Publications, 2017.
- Donges, J. F., Heitzig, J., Barfuss, W., Wiedermann, M., Kassel, J. A., Kittel, T., Kolb, J. J., Kolster, T., Müller-Hansen, F., Otto, I. M., Zim-  
585 merer, K. B., and Lucht, W.: Earth system modeling with endogenous and dynamic human societies: the copan: CORE open World–Earth modeling framework, *Earth System Dynamics*, 11, 395–413, <https://doi.org/10.5194/esd-11-395-2020>, publisher: Copernicus GmbH, 2020.
- Edwards, L. E.: What Is the Anthropocene?, <https://eos.org/opinions/what-is-the-anthropocene>, 2015.
- Fanning, A. L. and Raworth, K.: Doughnut of social and planetary boundaries monitors a world out of balance, *Nature*, 646, 47–56,   
590 <https://doi.org/10.1038/s41586-025-09385-1>, publisher: Nature Publishing Group, 2025.
- Folke, C., Carpenter, S. R., Walker, B., Scheffer, M., Chapin, T., and Rockström, J.: Resilience Thinking: Integrating Resilience, Adaptability and Transformability, *Ecology and Society*, 15, art20, <https://doi.org/10.5751/ES-03610-150420>, 2010.
- Franco-Gaviria, F., Amador-Jiménez, M., Millner, N., Durden, C., and Urrego, D. H.: Quantifying resilience of socio-ecological systems through dynamic Bayesian networks, *Frontiers in Forests and Global Change*, 5, 889 274, <https://doi.org/10.3389/ffgc.2022.889274>, 2022.
- 595 Hellmann, F., Schultz, P., Grabow, C., Heitzig, J., and Kurths, J.: Survivability of Deterministic Dynamical Systems, *Scientific Reports*, 6, 29 654, <https://doi.org/10.1038/srep29654>, 2016.
- IPCC: Climate Change 2023: Synthesis Report. Contribution of Working Groups I, II and III to the Sixth Assessment Report of the Intergovernmental Panel on Climate Change, IPCC, Geneva, Switzerland, <https://doi.org/10.59327/IPCC/AR6-9789291691647>, 2023.
- John, Y. J., Caldwell, L., McCoy, D. E., and Braganza, O.: Dead Rats, Dopamine, Performance Metrics, and Peacock Tails: Proxy Failure Is  
600 an Inherent Risk in Goal-Oriented Systems, *Behavioral and Brain Sciences*, 47, e67, <https://doi.org/10.1017/S0140525X23002753>, 2024.
- Kemp, L., Xu, C., Depledge, J., Ebi, K. L., Gibbins, G., Kohler, T. A., Rockström, J., Scheffer, M., Schellnhuber, H. J., Steffen, W., and Lenton, T. M.: Climate Endgame: Exploring catastrophic climate change scenarios, *Proceedings of the National Academy of Sciences*, 119, e2108146 119, <https://doi.org/10.1073/pnas.2108146119>, publisher: Proceedings of the National Academy of Sciences, 2022.
- Klein, A., Unverzagt, K., Alba, R., Donges, J. F., Hertz, T., Krueger, T., Lindkvist, E., Martin, R., Niewöhner, J., Prawitz, H., Schlüter,  
605 M., Schwarz, L., and Wijermans, N.: From situated knowledges to situated modelling: a relational framework for simulation modelling, *Ecosystems and People*, 20, 2361 706, <https://doi.org/10.1080/26395916.2024.2361706>, publisher: Taylor & Francis \_eprint: <https://doi.org/10.1080/26395916.2024.2361706>, 2024.
- Krakovská, H., Kuehn, C., and Longo, I. P.: Resilience of dynamical systems, *European Journal of Applied Mathematics*, 35, 155–200, <https://doi.org/10.1017/S0956792523000141>, 2024.
- 610 Lade, S. J., Haider, L. J., Engström, G., and Schlüter, M.: Resilience offers escape from trapped thinking on poverty alleviation, *Science Advances*, 3, e1603 043, <https://doi.org/10.1126/sciadv.1603043>, publisher: American Association for the Advancement of Science, 2017.
- Lebel, L., Anderies, J. M., Campbell, B., Folke, C., Hatfield-Dodds, S., Hughes, T. P., and Wilson, J.: Governance and the Capacity to Manage Resilience in Regional Social-Ecological Systems, *Ecology and Society*, 11, art19, <https://doi.org/10.5751/ES-01606-110119>, 2006.



- Lenton, T., Armstrong McKay, D., Loriani, S., Abrams, J., Lade, S., Donges, J., Buxton, J., Milkoreit, M., Powell, T., Smith, S. R., Zimm, C., Bailey, E., Dyke, J., Ghadiali, A., and Laybourn, L.: Global Tipping Points Report 2023, Tech. rep., Zenodo, <https://doi.org/10.5281/ZENODO.15188118>, 2023.
- Lenton, M., T., Milkoreit, M., Willcock, S., Abrams, F., J., Armstrong McKay, I., D., Buxton, E., J., Donges, F., J., Loriani, S., Wunderling, N., Alkemade, F., Barrett, M., Constantino, S., Powell, T., Smith, R., S., Boulton, A., C., Pinho, P., Dijkstra, H., Pearce-Kelly, P., Roman-Cuesta, M., R., and Dennis, D., eds.: The Global Tipping Points Report 2025, University of Exeter, Exeter, UK, <https://global-tipping-points.org/download/1419/>, 2025.
- Lenton, T. M., Held, H., Kriegler, E., Hall, J. W., Lucht, W., Rahmstorf, S., and Schellnhuber, H. J.: Tipping elements in the Earth's climate system, *Proceedings of the National Academy of Sciences*, 105, 1786–1793, <https://doi.org/10.1073/pnas.0705414105>, 2008.
- Lesk, C., Csala, D., Hasse, R., Sgouridis, S., Levesque, A., Mach, K. J., Horen Greenford, D., Matthews, H. D., and Horton, R. M.: Mitigation and adaptation emissions embedded in the broader climate transition, *Proceedings of the National Academy of Sciences*, 119, e2123486 119, <https://doi.org/10.1073/pnas.2123486119>, publisher: Proceedings of the National Academy of Sciences, 2022.
- Martin, S.: The cost of restoration as a way of defining resilience: a viability approach applied to a model of lake eutrophication, *Ecology and society*, 9, 2004.
- Menck, P. J., Heitzig, J., Marwan, N., and Kurths, J.: How basin stability complements the linear-stability paradigm, *Nature Physics*, 9, 89–92, <https://doi.org/10.1038/nphys2516>, publisher: Nature Publishing Group, 2013.
- Milkoreit, M.: Political science and the Earth system: Adapting governance to planetary realities, *The British Journal of Politics and International Relations*, 27, 551–565, <https://doi.org/10.1177/13691481251326418>, 2025.
- Milkoreit, M., Hodbod, J., Baggio, J., Benessaiah, K., Calderón-Contreras, R., Donges, J. F., Mathias, J.-D., Rocha, J. C., Schoon, M., and Werners, S. E.: Defining tipping points for social-ecological systems scholarship—an interdisciplinary literature review, *Environmental Research Letters*, 13, 033 005, <https://doi.org/10.1088/1748-9326/aaaa75>, 2018.
- Newman, R. and Noy, I.: The global costs of extreme weather that are attributable to climate change, *Nature Communications*, 14, 6103, <https://doi.org/10.1038/s41467-023-41888-1>, publisher: Nature Publishing Group, 2023.
- Nolan, B.: The Median Versus Inequality-Adjusted GNI as Core Indicator of ‘Ordinary’ Household Living Standards in Rich Countries, *Social Indicators Research*, 150, 569–585, <https://doi.org/10.1007/s11205-020-02311-0>, 2020.
- Raworth, K.: A Safe and Just Space for Humanity: Can we live within the doughnut?, Oxfam, ISBN 978-1-78077-059-8, google-Books-ID: tSikdAjHPf8C, 2012.
- Richardson, K., Steffen, W., Lucht, W., Bendtsen, J., Cornell, S. E., Donges, J. F., Drüke, M., Fetzer, I., Bala, G., Von Bloh, W., Feulner, G., Fiedler, S., Gerten, D., Gleeson, T., Hofmann, M., Huiskamp, W., Kummu, M., Mohan, C., Nogués-Bravo, D., Petri, S., Porkka, M., Rahmstorf, S., Schaphoff, S., Thonicke, K., Tobian, A., Virkki, V., Wang-Erlandsson, L., Weber, L., and Rockström, J.: Earth beyond six of nine planetary boundaries, *Science Advances*, 9, eadh2458, <https://doi.org/10.1126/sciadv.adh2458>, 2023.
- Ripple, W. J., Wolf, C., Gregg, J. W., Rockström, J., Mann, M. E., Oreskes, N., Lenton, T. M., Rahmstorf, S., Newsome, T. M., Xu, C., Svenning, J.-C., Pereira, C. C., Law, B. E., and Crowther, T. W.: The 2024 state of the climate report: Perilous times on planet Earth, *BioScience*, 74, 812–824, <https://doi.org/10.1093/biosci/biae087>, 2024.
- Robinson, A., Calov, R., and Ganopolski, A.: Multistability and critical thresholds of the Greenland ice sheet, *Nature Climate Change*, 2, 429–432, <https://doi.org/10.1038/nclimate1449>, publisher: Nature Publishing Group, 2012.
- Rockström, J., Steffen, W., Noone, K., Persson, A., Chapin, F. S., Lambin, E. F., Lenton, T. M., Scheffer, M., Folke, C., Schellnhuber, H. J., Nykvist, B., de Wit, C. A., Hughes, T., van der Leeuw, S., Rodhe, H., Sörlin, S., Snyder, P. K., Costanza, R., Svedin, U., Falkenmark,



- M., Karlberg, L., Corell, R. W., Fabry, V. J., Hansen, J., Walker, B., Liverman, D., Richardson, K., Crutzen, P., and Foley, J. A.: A safe operating space for humanity, *Nature*, 461, 472–475, <https://doi.org/10.1038/461472a>, publisher: Nature Publishing Group, 2009.
- 655 Rockström, J., Beringer, T., Hole, D., Griscom, B., Mascia, M. B., Folke, C., and Creutzig, F.: We need biosphere stewardship that protects carbon sinks and builds resilience, *Proceedings of the National Academy of Sciences*, 118, e2115218118, <https://doi.org/10.1073/pnas.2115218118>, 2021.
- Rockström, J., Gupta, J., Qin, D., Lade, S. J., Abrams, J. F., Andersen, L. S., Armstrong McKay, D. I., Bai, X., Bala, G., Bunn, S. E., Ciobanu, D., DeClerck, F., Ebi, K., Gifford, L., Gordon, C., Hasan, S., Kanie, N., Lenton, T. M., Loriani, S., Liverman, D. M., Mohamed, A., Nakicenovic, N., Obura, D., Ospina, D., Prodan, K., Rammelt, C., Sakschewski, B., Scholtens, J., Stewart-Koster, B., Tharammal, 660 T., Van Vuuren, D., Verburg, P. H., Winkelmann, R., Zimm, C., Bennett, E. M., Bringezu, S., Broadgate, W., Green, P. A., Huang, L., Jacobson, L., Ndehedehe, C., Pedde, S., Rocha, J., Scheffer, M., Schulte-Uebbing, L., De Vries, W., Xiao, C., Xu, C., Xu, X., Zafra-Calvo, N., and Zhang, X.: Safe and just Earth system boundaries, *Nature*, 619, 102–111, <https://doi.org/10.1038/s41586-023-06083-8>, 2023.
- Said, N. and Wöfl, V.: Impact of Constructive Narratives About Climate Change on Learned Helplessness and Motivation to Engage in 665 Climate Action, *Environment and Behavior*, 57, 75–117, <https://doi.org/10.1177/00139165251315576>, publisher: SAGE Publications Inc, 2025.
- Scheffer, M. and Carpenter, S. R.: Catastrophic regime shifts in ecosystems: linking theory to observation, *Trends in Ecology & Evolution*, 18, 648–656, <https://doi.org/10.1016/j.tree.2003.09.002>, 2003.
- Scheffer, M. and Van Nes, E. H.: Shallow lakes theory revisited: various alternative regimes driven by climate, nutrients, depth and lake size, 670 *Hydrobiologia*, 584, 455–466, <https://doi.org/10.1007/s10750-007-0616-7>, 2007.
- Scheffer, M., Hosper, S. H., Meijer, M.-L., Moss, B., and Jeppesen, E.: Alternative equilibria in shallow lakes, *Trends in Ecology & Evolution*, 8, 275–279, [https://doi.org/10.1016/0169-5347\(93\)90254-M](https://doi.org/10.1016/0169-5347(93)90254-M), 1993.
- Scheffer, M., Bascompte, J., Brock, W. A., Brovkin, V., Carpenter, S. R., Dakos, V., Held, H., Van Nes, E. H., Rietkerk, M., and Sugihara, G.: Early-warning signals for critical transitions, *Nature*, 461, 53–59, <https://doi.org/10.1038/nature08227>, 2009.
- 675 Scheffer, M., Carpenter, S. R., Dakos, V., and Van Nes, E. H.: Generic Indicators of Ecological Resilience: Inferring the Chance of a Critical Transition, *Annual Review of Ecology, Evolution, and Systematics*, 46, 145–167, <https://doi.org/10.1146/annurev-ecolsys-112414-054242>, 2015.
- Schellnhuber, H. J.: ‘Earth system’ analysis and the second Copernican revolution, *Nature*, 402, C19–C23, <https://doi.org/10.1038/35011515>, publisher: Nature Publishing Group, 1999.
- 680 Schleussner, C.-F., Ganti, G., Rogelj, J., and Gidden, M. J.: An emission pathway classification reflecting the Paris Agreement climate objectives, *Communications Earth & Environment*, 3, 135, <https://doi.org/10.1038/s43247-022-00467-w>, publisher: Nature Publishing Group, 2022.
- Schultz, P., Menck, P. J., Heitzig, J., and Kurths, J.: Potentials and limits to basin stability estimation, *New Journal of Physics*, 19, 023 005, <https://doi.org/10.1088/1367-2630/aa5a7b>, publisher: IOP Publishing, 2017.
- 685 Sinha, A., Venkatesh, A., Jordan, K., Wade, C., Eshraghi, H., de Queiroz, A. R., Jaramillo, P., and Johnson, J. X.: Diverse decarbonization pathways under near cost-optimal futures, *Nature Communications*, 15, 8165, <https://doi.org/10.1038/s41467-024-52433-z>, publisher: Nature Publishing Group, 2024.



- Steffen, W., Rockström, J., Richardson, K., Lenton, T. M., Folke, C., Liverman, D., Summerhayes, C. P., Barnosky, A. D., Cornell, S. E., Crucifix, M., Donges, J. F., Fetzer, I., Lade, S. J., Scheffer, M., Winkelmann, R., and Schellnhuber, H. J.: Trajectories of the Earth System  
690 in the Anthropocene, *Proceedings of the National Academy of Sciences*, 115, 8252–8259, <https://doi.org/10.1073/pnas.1810141115>, 2018.
- Tamberg, L. A., Heitzig, J., and Donges, J. F.: A modeler’s guide to studying the resilience of social-technical-environmental systems, *Environmental Research Letters*, 17, 055 005, <https://doi.org/10.1088/1748-9326/ac60d9>, publisher: IOP Publishing, 2022.
- Van Kan, A., Jegminat, J., Donges, J. F., and Kurths, J.: Constrained basin stability for studying transient phenomena in dynamical systems, *Physical Review E*, 93, 042 205, <https://doi.org/10.1103/PhysRevE.93.042205>, 2016.
- 695 Winkelmann, R., Dennis, D., Donges, J. F., Loriani, S., Klose, A. K., Abrams, J. F., Alvarez-Solas, J., Albrecht, T., McKay, D. A., Bathiany, S., Navarro, J. B., Brovkin, V., Burke, E., Danabasoglu, G., Donner, R. V., Druke, M., Georgievski, G., Goelzer, H., Harper, A. B., Hegerl, G., Hirota, M., Hu, A., Jackson, L. C., Jones, C., Kim, H., Koenigk, T., Lawrence, P., Lenton, T. M., Liddy, H., Licón-Saláiz, J., Menthon, M., Montoya, M., Nitzbon, J., Nowicki, S., Otto-Bliesner, B., Pausata, F., Rahmstorf, S., Ramin, K., Robinson, A., Rockström, J., Romanou, A., Sakschewski, B., Schädel, C., Sherwood, S., Smith, R. S., Steinert, N. J., Swingedouw, D., Willeit, M., Weijer, W., Wood,  
700 R., Wyser, K., and Yang, S.: The Tipping Points Modelling Intercomparison Project (TIPMIP): Assessing tipping point risks in the Earth system, *Earth System Dynamics Discussions*, <https://doi.org/10.5194/egusphere-2025-1899>, 2025.
- World Bank: World Bank Country and Lending Groups – World Bank Data Help Desk, <https://datahelpdesk.worldbank.org/knowledgebase/articles/906519-world-bank-country-and-lending-groups>, 2025.
- Wunderling, N., Winkelmann, R., Rockström, J., Loriani, S., Armstrong McKay, D. I., Ritchie, P. D. L., Sakschewski, B., and Donges,  
705 J. F.: Global warming overshoots increase risks of climate tipping cascades in a network model, *Nature Climate Change*, 13, 75–82, <https://doi.org/10.1038/s41558-022-01545-9>, publisher: Nature Publishing Group, 2023.
- Wunderling, N., von der Heydt, A. S., Aksenov, Y., Barker, S., Bastiaansen, R., Brovkin, V., Brunetti, M., Couplet, V., Kleinen, T., Lear, C. H., Lohmann, J., Roman-Cuesta, R. M., Sinet, S., Swingedouw, D., Winkelmann, R., Anand, P., Barichivich, J., Bathiany, S., Baudena, M., Bruun, J. T., Chiessi, C. M., Coxall, H. K., Docquier, D., Donges, J. F., Falkena, S. K. J., Klose, A. K., Obura, D., Rocha, J.,  
710 Rynders, S., Steinert, N. J., and Willeit, M.: Climate tipping point interactions and cascades: a review, *Earth System Dynamics*, 15, 41–74, <https://doi.org/10.5194/esd-15-41-2024>, publisher: Copernicus GmbH, 2024.
- Yi, C., Rietkerk, M., Anderies, J. M., Chen, D., Dakos, V., Ritchie, P. D. L., Rocha, J. C., Milkoreit, M., and Quinn, C.: Principles for guiding future research on resilience and tipping points, *Environmental Research Letters*, 20, 031 008, <https://doi.org/10.1088/1748-9326/adb7f3>, publisher: IOP Publishing, 2025.